Utilizing Shape-Memory-Alloys to Enhance the Performance and Safety of Civil Infrastructure: a Review

M. S. Alam
Ph.D. Candidate, Department of Civil and Environmental Engineering,
The University of Western Ontario
London, ON, Canada N6A 5B9

M. A. Youssef
Assistant Professor, Department of Civil and Environmental Engineering,
The University of Western Ontario
London, ON, Canada N6A 5B9

M. Nehdi
Associate Professor, Department of Civil and Environmental Engineering,
The University of Western Ontario
London, ON, Canada N6A 5B9

Corresponding Author: **M. Nehdi**
Associate Professor, Department of Civil and Environmental Engineering,
The University of Western Ontario,
London, Ontario, Canada, N6A 5B9
Email: mnehdi@eng.uwo.ca,
Fax: 519-661-3779, Phone: 519-661-2111, Ext.: 88308.

Word Count: 10,280

Abstract: Shape-Memory-Alloys (SMAs) are special materials with a substantial potential for various civil engineering applications. The novelty of such materials lies in their ability to undergo large deformations and return to their undeformed shape through stress removal (superelasticity) or heating (shape-memory-effect). In particular, SMAs have distinct thermo-mechanical properties including: superelasticity, shape-memory-effect, and hysteretic damping. These properties could be effectively utilized to substantially enhance the safety of various structures. Although the high cost of SMAs is still limiting their use, research investigating their production and processing is expected to make it more cost-competitive. Thus, it is expected that SMAs will emerge as an essential material in the construction industry. This paper examines the fundamental characteristics of SMAs, its constitutive material models and the factors influencing its engineering properties. Some of the potential applications of SMAs are discussed including the reinforcement and repair of structural elements, prestress applications, and the development of kernel components for seismic devices such as dampers and isolators. The paper synthesises existing information on the properties of SMAs summarized in concise and useful tables, and explains different alternatives for its application, which should motivate researchers and practicing engineers to extend its use in novel and emerging applications.

Keywords: shape-memory-alloy, superelasticity, shape-memory-effect, construction, retrofitting.

1. Introduction

Civil infrastructure constitutes a substantial portion of the national wealth in most countries. Because of aging and decay, it often needs monitoring, evaluation and repairing at regular time intervals. This has resulted in infrastructure management becoming an economic burden. It is argued that if a structure is made smart and capable to detect its own damage, repair its condition and adopt changes in its loading conditions, many problems related to infrastructure management could be eliminated. This thinking has recently given rise to smart materials and structures, which are intended to adapt to the surrounding environment, provide optimal operating conditions, minimize energy use, enhance overall life cycle performance, and significantly reduce maintenance costs (Ullakko 1996).

Shape-Memory-Alloys (SMAs) are unique materials that have the ability to undergo large deformation and return to a predetermined shape upon unloading or by heating. The distinct and unique properties of SMAs make them intelligent materials having the potential to be used in building smart structures that respond and adapt to changes in condition or environment (Hardwicke 2003). SMAs have been used in a wide variety of applications in different fields and industries such as aviation, medical equipment and implants. They have also been used as actuators, switches, valves and clamping devices. SMAs are gradually gaining recognition and finding new applications in medical sciences (Miller 2005) and in several engineering fields (Norton 1998; Jung 2006).

There are numerous applications of SMAs in civil engineering (Janke et al. 2005). Some of these applications, especially in the seismic field, have been discussed by DesRoches and Smith (2004); Wilson and Wesolowsky (2005) and Song et al. (2006). Wilson and Wesolowsky (2005) and DesRoches and Smith (2004) provided detailed description of experiments conducted

by various researchers on the mechanical properties of SMA, but did not summarize the associated results. Wilson and Wesolowsky (2005) and Janke et al. (2005) provided data on the tensile properties of SMAs, whereas other mechanical properties of SMA under compression, shear and torsion were not included in their study; such properties are necessary for the design and analysis of structures. None of the studies mentioned above provided clear direction on using built-in SMA models existing in finite element (FE) packages so that practicing engineers can readily use such models to analyze structures using SMA materials.

The current paper presents, in a systematic manner, a summary of the basic characteristics of SMAs, some useful tables on their mechanical properties, and a critical review of the state-of-art of their possible seismic and non-seismic applications along with their future expected trends in civil engineering. This paper also provides a general description on the modelling aspects of SMAs in addition to useful information for practicing engineers on built-in SMA models available in some FE packages. Over the last two decades, a substantial amount of research has been done on the material science and possible uses of SMAs in structural applications. It is being realized that SMAs possess a substantial potential to replace or complement conventional materials, while achieving great gains in performance and safety.

2. Fabrication of SMAs

Several SMAs with various compositions have been developed. These include Ag-Cd, Au-Cd, Cu-Zn, Cu-Zn-Al, Cu-Al-Ni, Fe-Mn, Mn-Cu, Fe-Pd, Cu–Zn–Al–Mn–Zr, Cu–Al–Be, Ti-Ni-Cu, Ti-Ni-Hf, Ni-Ti-Fe and Ni-Ti, etc. (Otsuka and Wayman 1999). SMAs are usually fabricated by melting alloys in a high vacuum or inert gas environment to avoid contamination since the melted alloy may be reactive with oxygen. The alloys are then hot worked or cold

worked to the desired shape, e.g. wire, ribbon, tube, sheet, or bar. The final stage of the fabrication process is the shape-memory-treatment that characterizes SMA distinctively from other structural metals, in which alloys undergo appropriate thermomechanical processing to exhibit shape-memory-effect and superelasticity. Usually, the heat treatment temperature is kept below the recrystallization temperature of the alloy for shape memorization (Khantachawana et al. 1999). It should be noted that the cold worked alloys respond more reliably to the shape setting heat treatment than the hot worked alloys. This results in a finished shape with enhanced mechanical properties (Hodgson 2000).

3. Transformation temperatures

Like many other alloys and metals, SMA exhibits polymorphism, i.e. it possesses more than one crystal structure having the same chemical composition. The predominant crystal structure or phase in a polycrystalline metal depends on both stress and temperature and is controlled by both chemical composition and thermomechanical processing (Dolce and Cardone 2001). At a relatively low temperature, SMA exists in the martensite phase. When heated, it undergoes a transformation to the austenite phase (crystalline change). In the stress-free state, SMA is characterized by four distinct transformation temperatures (Fig. 1): martensite start (M_s), martensite finish (M_f), austenite start (A_s), and austenite finish (A_f). Typical values of transformation temperatures for several alloys in a stress-free state are presented in Table 1. SMA exists in a fully martensite state when its temperature (T) is less than M_f, and in a fully austenite state when T is greater than A_f. During the phase change from martensite-to-austenite and vice versa, both martensite and austenite phases coexist. The phase transformation of SMA during heating and cooling is qualitatively shown in Fig. 1. When the material is heated to A_s, its

phase starts to change gradually from martensite to austenite. At a temperature of A_f, this transformation is complete. Cooling the material will result in a phase change from 100% austenite at a temperature greater than M_s to 100% martensite when temperature M_f is reached. If the temperature in the austenite phase increases above M_d ($T>>A_f$), the superelasticity is lost.

A small change in the relative proportion of the constitutive metals can have a marked effect on the transformation temperatures (Table 1). It has been observed that under the same fabrication process, a one percent shift in the nickel content results in a 100°C change in the M_s or A_s point (Otsuka and Wayman 1999). Variation in the fabrication process of the alloys also significantly affects the transformation temperature even for the same chemical composition, as shown in Table 1.

4. Mechanical properties of SMAs

Each SMA considerably differs in its mechanical properties. Such properties vary over a wider range, not only due to variation in chemical composition, but also due to the atomic arrangement in the martensite and austenite phase of the SMA that depends on the thermomechanical processing and heat treatment. Even a slight change in the relative proportion of the constitutive metals within the same alloy may significantly affect its mechanical properties (Strnadel et al. 1995). Various SMAs in the form of wires and bars with different diameters have been tested by a number of researchers under tensile, compressive, torsional and shearing forces. The various parameters defining the material properties are presented in Table 2 for the most widely used SMA (i.e. Ni-Ti), and in Table 3 for some other SMAs.

4.1 Tensile and compressive behaviour

A typical stress-strain curve of SMA (austenite or martensite) under tensile and compressive forces is presented in Fig. 2. The curve is composed of four linear branches that are connected by smooth curves. For simplicity, the linear branches will be assumed to intersect as shown by the dotted lines in Fig. 2. The material is tested under both tensile and compressive forces (Liu et al. 1998). The length to diameter ratio was reduced in the case of specimens tested under compression compared to those in tension in order to avoid buckling. The material behaves elastically at the start of the test with a modulus of elasticity E_y until it reaches the yield stress, f_y. As it crosses f_y, there is a significant reduction in stiffness, where the modulus of elasticity, E_{P1} reduces to about 10 to 15% of E_y. Such stiffness is maintained up to a stress of f_{P1} and strain of ε_{P1}. As soon as it passes ε_{P1}, the specimen becomes stiffer and its modulus of elasticity E_{P2} reaches about 50 to 60% of E_y. Another yield point, f_{P2} occurs at a strain of ε_{P2}, which is followed by a yield plateau with a modulus of elasticity E_u (3 to 8% of E_y) until failure occurs by reaching the ultimate stress, f_u at a strain of ε_u. Typical values of characteristic axial strains (ε), axial stresses (f) and Young's modulus (E_y) are shown in Table 2 and 3.

4.2 Torsion and shear behaviour

The typical stress-strain curve of SMA under torsion and shear follows a similar pattern to that of the stress-strain curve under tension. The characteristic parameters of shear stress (τ), shear strain (γ), and shear modulus (G) are denoted by: τ_y, τ_{P1}, τ_{P2}, τ_u, γ_y, γ_{P1}, γ_{P2}, γ_u, G_y, G_{P1}, G_{P2} and G_u.

5. Unique properties of SMA

The shape-memory-effect (SME), superelasticity (PE), and performance under cyclic loading make SMA distinctive compared to other metals and alloys.

5.1. Shape-memory-effect

The stress-induced behaviour of SMA depends on temperature. In the martensite state ($T \leq A_s$), there will remain some residual-strain (ε) upon unloading. This is mainly due to the reorientation of twin variants of atoms as shown in Fig. 1. This residual-strain will theoretically completely disappear if the SMA is heated above A_f as shown by the curve in the strain-temperature plane of Fig. 3. Upon heating, the atoms reassemble themselves and the material regains its original shape, a phenomenon commonly known as shape-memory-effect (SME).

5.2. Superelasticity

In the austenite state ($T \geq A_f$) when SMA is loaded and unloaded, six distinctive characteristics can be recognized in the stress strain diagram (curve 2 of Fig. 3): (a) elastic response of austenite at low strains (<1%) as denoted by BC, (b) stress-induced transformation from austenite to martensite with a long and constant stress plateau at intermediate and large strains (1-6%) as indicated by CD, (c) elastic response in the stress-induced martensite state at large strains (>8%) represented by DE, (d) elastic recovery of strain upon stress removal as shown by EF, (e) instinctive recovery of strain at almost a constant stress path because of the reverse transformation to austenite due to the instability of martensite at $T > A_f$ as depicted by FG, and finally (f) elastic recovery in the austenite phase as indicated by GB (Wilson and Wesolowsky 2005). This exceptional property of SMA with the ability of recovering substantial

inelastic deformation upon unloading yields a characteristic hysteresis loop, which is known as superelasticity/pseudoelasticity (PE). If temperature in the austenite phase exceeds the maximum temperature at which martensite occurs (M_d) then PE of SMA is completely lost and it behaves like an elastic-plastic material as shown in curve 3 of Fig. 3.

5.3. Behaviour under repeated/cyclic loading

The unique properties of SMA under cyclic load have made it attractive for various engineering applications. Several researchers have tested the cyclic properties under tension, compression, shear and torsion of different SMAs. The typical stress-strain diagram of austenite-SMA under cyclic axial, shear and torsion forces are presented in Fig. 4, and those for martensite-SMA under cyclic axial and torsion forces are presented in Fig. 5.

When an SMA specimen is subjected to a cycle of deformation within its superelastic strain range, it dissipates a certain amount of energy without permanent deformation. This results from the phase transformation from austenite to martensite during loading and the reverse transformation during unloading ensuring a net release of energy. When SMA is loaded in the martensite phase, it yields at a nearly constant stress after initial elastic deformation and displays strain hardening at larger strains. When unloaded there remains some residual-strain at zero stress. This martensitic composition of SMA generates a full hysteresis loop around the origin (Fig. 5). Thus, martensite-SMA dissipates a much higher amount of energy compared to that of austenite-SMA due to its larger hysteresis loop. In the martensite phase under tension-compression cycles, the maximum stress attained in compression has been found to be approximately twice that in tension (Fig. 5). This may be due to the difference in the cyclic hardening and softening process that takes place in tension-compression at maximum and zero

strain, respectively (Liu et al. 1999). However, it needs to be mentioned that martensite is not self-balanced. Although superelastic-SMA dissipates less amount of energy compared to martensitic-SMA, its advantage is that it can still dissipate a considerable amount of energy under repeated load cycles with negligible residual-strain.

It can be observed that under shear stress, superelastic-SMA has some residual-strain after unloading, which may be due to the presence of some partially stabilized martensite (Orgeas et al. 1997). The mechanical behaviour of SMA under torsion slightly depends on the loading frequency in the superelastic range, but is independent in the case of the martensite phase. It has been found that in austenite and martensite phases, SMA exhibits highly stable and repeatable hysteresis under torsion (Dolce and Cardone 2001).

Generally, the loading plateau and the hysteretic loop gradually decrease and the residual-strain increases for successive loading cycles of a pseudoelastic SMA due to localized slip, which facilitates the formation of stress induced martensite. However, this behaviour has been proven to decrease and stabilize at a large number of cycles (Miyazaki et al. 1986). The strain rate also has an important effect on the mechanical properties of SMA. Increased strain rate causes an increase in stresses for both cases of loading and unloading with a narrow resultant hysteretic loop, thus resulting in an overall decrease in the energy dissipation capacity. This is mainly due to self-heating of the specimen during cycling, requiring a larger stress to induce a martensitic state.

6. Constitutive material modelling of SMA

Over the last decade, the use of SMA has emerged into a variety of fields such as medical sciences, aerospace, mechanical and civil engineering. Therefore, the development of proper

constitutive models has become an important prerequisite in modelling and designing SMA devices before reaching the prototype stage in the design process. The peculiar thermomechanical behaviour of SMA with SME and PE has made constitutive modelling a three-dimensional complex problem since it is difficult to choose suitable tensorial variables to express the behaviour of SMA under multiaxial responses. SMAs are usually modelled following either a phenomenological or a thermodynamics approach.

6.1 Phenomenological modelling

Since most civil engineering applications of SMA are related to the use of bars and wires, one-dimensional phenomenological models (PMs) are often considered suitable. In phenomenological models, the parameters shown in Figs. 1 and 2 are defined experimentally. Several researchers have proposed uniaxial phenomenological models (Tanaka and Nagaki 1982; Liang and Rogers 1990 and others).

The superelastic behaviour of SMA has been incorporated in a number of finite element packages e.g. ANSYS 10.0 (ANSYS Inc. 2005), ABAQUS 6.4 (Hibbitt et al. 2003) and Seismostruct (2004) where the material models are included from Auricchio et al. (1997), Auricchio and Taylor (1996), and Auricchio and Sacco (1997), respectively. The parameters used to define the material models in FE software packages include: 1) austenite-to-martensite starting stress (f_y); 2) austenite-to-martensite finishing stress (f_{P1}); 3) martensite-to-austenite starting stress (f_{T1}); 4) martensite-to-austenite finishing stress (f_{T2}); 5) superelastic plateau strain length or maximum residual-strain (ε_l); 6) modulus of elasticity for martensite and austenite phases (E_a and E_s); and 7) the ratio of the transformation stresses (α) under tension and

compression. Figure 6 shows the 1D-superelastic model used in ANSYS 10.0 where SMA has been subjected to multiple stress cycles at a constant temperature.

6.2. Thermodynamics-based modelling

Thermodynamics-based models (TMs) are built on the laws of thermodynamics and energy considerations. A number of TMs have been developed illustrating one or more aspects of SMAs. Patoor et al. (1994), Goo and Lexcellent (1997), Huang and Brinson (1998), and others adopted micromechanics approaches and pursued closely crystallographic phenomena within the material using thermodynamics laws.

TMs are much more complicated and computationally demanding than PMs as they present a highly sensible technique to derive precise three-dimensional constitutive laws. However, PMs seem to be more adequate for civil engineering applications involving SMA wires and bars since they can be easily incorporated in FE programs.

7. Applications of SMA

The unique characteristics of SMAs have led to several applications in civil engineering. In this section, an attempt has been made to examine these applications in both newly built structures and retrofitted structures.

7.1 SMA in new structures

Substantial research has been conducted on the use of SMA in the construction of new structures in the form of reinforcement, bolted connections, restrainers, bracings, and prestressing strands.

7.1.1. Reinforcement in concrete structures

Bridges and buildings in seismic regions are susceptible to severe damage due to excessive lateral displacements. Earthquake resistant structures should be designed to behave elastically under moderate earthquakes. Under strong ground motions, it is not economically feasible to build structures that will perform elastically. In conventional seismic design, steel is expected to yield in order to dissipate energy while undergoing permanent deformation. Conversely, if SMA is used as reinforcement, it will yield when subjected to high seismic loads, but will not retain significant permanent deformations (Wang 2004).

The seismic performance of RC columns with superelastic-SMA rebar in the plastic hinge area was investigated by Wang (2004). Two quarter-scale spirally tied RC circular columns with SMA (Ni-Ti) in the plastic hinge area and steel rebar in other areas were designed, constructed and tested using a shake table. It was observed that SMA-RC columns were superior to conventional steel-RC columns in limiting relative column top displacement and residual-displacements and withstanding larger earthquake amplitudes. After the test, the damaged SMA RC column specimen was repaired with engineering cementitious composites and retested using the same approach of the initial test. The shake table data showed that the repaired SMA RC column performed better than the original intact specimen in terms of force-displacement capacity and ductility.

7.1.2 Bolted joints

Beam-column and column-foundation joints are often the weakest link of a structure during earthquake events. Superelastic-SMA materials can be effectively employed in such joints

in order to reduce their vulnerability by dissipating greater energy through large plastic deformation and then recovering it.

Ocel et al. (2004) investigated the effectiveness of partially restrained steel beam-column connections using SMA elements. The connection consisted of four large diameter Ni-Ti tendons in martensite phase connecting the beam flange to the column flange serving as the primary moment transfer mechanism. Two full-scale connections were tested. The connections exhibited a high level of energy dissipation, large ductility capacity, and no strength degradation after being subjected to load cycles up to 4% drift. After the initial testing series, the tendons were heated to recover the residual beam tip-displacements. After initiating SME within the tendons, the connections were retested, displaying repeatable and stable hysteretic behaviour. An additional test was performed under dynamic loading, which showed a similar behaviour, except for a decrease in energy dissipation capacity compared to that observed in quasi-static tests. This proof-of-concept indicates a potential for the use of SMA in seismic design and retrofit of structures.

When a fastener is tightened, it is subjected to tension commonly known as preload. PE of SMA can also be utilized to regain preload drop in bolted joints, and thus provide the necessary clamping force to keep joint members together. Hesse et al. (2004) used martensite-SMA (Ni-Ti) rings to repair loose bolted joints. The axial force in the SMA ring was continuously monitored, and if decreased, the ring was heated above A_f to increase its dimension axially, thus providing a means of tightening the joint. The advantage of using SMA ring lies in the fact that unlike other metals, its dimension will not decrease with the temperature drop as long as its temperature remains above M_s as shown in Fig. 1. Thus, SMA rings can help in the self-healing of bolted joints.

7.1.3. Bracings

Salichs et al. (2001) conducted a numerical study with a one-storey prototype-building model strengthened with superelastic-SMA (Ni-Ti) diagonal bracing wires subjected to a harmonic base excitation. The results showed that additional damping provided by superelastic-SMA hysteresis reduced the peak displacement and prevented damage compared to that of steel bracing with similar stiffness. Due to a lower level of damage, this should also make the repair of frames easier even after a severe earthquake.

7.1.4. Prestressing

Prestressing concrete and masonry structures with SMA strands/wires has been found to be a viable alternative. Both pretensioning and post-tensioning can be done using SMA. The benefits of employing SMAs in prestressing include a) active control on the amount of prestressing with increased additional load carrying capacity, b) no involvement of jacking or strand-cutting, and c) no elastic-shortening, friction and anchorage-losses over time.

Pretensioning

Pretensioned SMA strands/wires in the martensite state are embedded in concrete, then electrically heated to transform from martensite-to-austenite phase, thus undergoing large shrinkage strains; if constrained, it generates a significant prestressing force in concrete. The application of conventional prestressing by pretensioning wires requires jacking and release of prestressing strands, which may cause cracking at the end of girders during strand-cutting (Kannel et al. 1997). If SMA is used for prestressing, it requires no jacking or strand-cutting. For

instance, Maji and Negret (1998) used Ni-Ti strands for prestressing concrete beams by utilizing SME of SMAs. SMA wire-strands developed good bonding strength to concrete by mechanical interlocking where the strands transferred stresses to the concrete beam even beyond their yield stress. The test indicated a potential for creating smart structures where the amount of prestressing can be increased or decreased as required. Such structures could for instance actively accommodate additional loading or remedy prestress losses over time.

Post-tensioning

Pre-stretched SMA strands/tendons in the martensite phase are passed through post-tensioning ducts after placement of concrete, and heating can conveniently induce post-tensioning. Post tensioning requires anchoring of SMA bars, but does not require jacking and strand-cutting, which mitigates the possibility of friction and anchorage-losses. Prestressing-losses due to elastic-shortening, creep, and shrinkage are negligible and can be recovered by heating SMA bars when required.

El-Tawil and Ortega-Rosales (2004) used SMA tendons to permanently prestress concrete. Two types of SMA were investigated: Ni-Ti and Ni-Ti-Nb alloys. The former SMA was found unsuitable for permanent prestressing applications because all recovery-stresses were lost due to temperature drop after the heat source was removed. It was assumed that the material might have been overheated and entered into its annealing temperature. The latter alloy proved to be a better solution for permanent prestress applications with a slight drop in the recovery-stress. However, its recovery-stress was rather low (156 to 244 MPa) compared to that of the Ni-Ti alloy (275 to 380 MPa). The constrained recovery-stress was found to increase mildly with the pre-strain level. Ni-Ti-Nb tendons were pre-strained and placed in mortar beams. After beam

curing, the tendons were heat-triggered to induce post-tensioning. Four-point bending tests on beams demonstrated that significant prestressing was achieved.

It is to be noted that for permanent prestressing, whether it is pretensioning or post-tensioning, A_f should be above the ambient temperature (T_a) to prevent accidental activation of SMA during construction. Also, the M_s should be below the lowest operating temperature for the prestressing to be active during operation.

7.1.5. Restrainers

One of the major problems of bridges during earthquakes is their unseating due to excessive relative hinge opening and displacement (Schiff 1998). Limitations of existing unseating prevention devices include small elastic strain range, limited ductility, and no recentering capability (ability to bring the member back to its original position even after inelastic deformation). These limitations can be overcome by introducing SMA restrainers. For instance, DesRoches and Delemont (2002) evaluated the efficacy of SMA restrainer bars through an analytical study of a multi-span simply supported bridge subjected to a set of ground motion records. The performance of SMA restrainers was compared with that of conventional steel restrainers. The results demonstrated that SMA restrainers were capable of reducing relative hinge displacements much more effectively than conventional restrainers.

7.2. SMA in retrofitting of existing structures

Inadequate design, faulty construction, impact and dynamic loading, and time-dependent deformation are among the various reasons for which a structure or one of its elements can become deficient to withstand the applied loads and risk failure. Steel and fibre-reinforced-

polymer (FRP) are commonly used for retrofitting deficient structures. SMA is another potential candidate for such applications having several advantages over steel and FRP. If SMA is used as a retrofitting material instead of steel and FRP, structural forces can be reapplied in case of elastic deformation, lost torque or slippage. Another important property of superelastic-SMA materials is its recentering capability, which may be utilized in the form of bracings and dampers for retrofitting structures in earthquake prone zones. Moreover, SMA is highly resistant to corrosion compared to steel. In the case of FRP, it is brittle and vulnerable to fire, whereas SMA is ductile with relatively higher resistance to fire and its strength increases as the temperature increases up to a certain limit.

7.2.1. Bracings

A shaking table test program was carried out by Cardone et al. (2004) to evaluate the effectiveness of passive control bracing systems for the seismic retrofitting of RC frames designed for gravity loads. The hysteretic dissipating capacity of steel and superelastic property of SMA based bracing devices were used for retrofitting. A four-storey (305 cm high) 3D ¼-scale RC frame model with two longitudinal bays (231 cm long) and one transverse bay (133 cm wide) was used. The SMA brace was made of superelastic-SMA wires fitted inside two concentric steel tubes tending to move relatively to each other producing double-flag-shaped hysteresis loops. The test variables considered in the shake table tests were a bare frame model, steel-braced frame model, SMA-braced frame model, unidirectional motion, bi-directional motion, centered and eccentric masses. For the retrofitted SMA-based braced frame, the natural frequency was found to be distinctly higher than that measured for the steel-based braced frame in spite of using larger steel sections. This was mainly due to the strong effect on the initial

stiffness of steel braces by the flexibility of dissipating components, while SMA braces coincided with the axial stiffness of the steel tubes due to wire pretensioning. The experimental results confirmed the great potential and practical feasibility of using SMA-based braces in frame structures, which are characterized by greater initial stiffness and lower weight, and more importantly a recentering capability, compared to steel braces.

7.2.2. Prestressing

An early practical use of SMA in the rehabilitation of a real structure is the work of Indirli et al. (2001). The Trignano S. Giorgio Church built in 1302 in Italy is an ancient structure, which was seriously damaged by a 4.8 Richter magnitude earthquake on October 15, 1996. The masonry column supported bell tower within the church was critically damaged and needed to be retrofitted. To increase the flexural resistance of the tower, four vertical prestressing steel tie bars with four post-tensioned SMA devices connected in series were anchored at the roof and foundation in the internal corners of the structure. SMA devices insured that the force applied to the masonry is maintained at a compressive level of 20 kN (axial capacity of the masonry column). Each SMA device included sixty superelastic-SMA wires of 1 mm diameter and 300 mm length. The performance of the innovative rehabilitation scheme was positively verified after the tower was shaken by another 4.5 Richter magnitude earthquake. No forms of distress or damage were noticed after the shock.

Soroushian et al. (2001) used iron-based SMA bars for the rehabilitation of deficient bridge girders. The martensite-SMA bars were pre-elongated and anchored to the deficient structural element. Upon electrical resistance heating and transforming to austenite, the constraint shape recovery caused transfer of corrective forces to the structure. The approach was

verified by testing a RC beam that was deficient in shear. After loading, beam shear cracks occurred. The RC beam was subsequently repaired through post-tensioning with SMA rods and tested to failure. The results showed that the initial ductility and load carrying capacity of the rehabilitated beam were almost fully regained. The practical demonstration of this repairing approach was applied in a bridge in Michigan, which was lacking in shear strength and suffered some cracks in T-beams extending into the deck. The repair process involved local post-tensioning of the cracked region with SMA rods and could successfully reduce the average crack width by about 40%. The main advantage of this repair scheme over the conventional prestressing technique is that in case of slip or elastic deformation the corrective forces to the structural system can be reapplied simply by heating the installed SMA rods.

7.3. Dampers and isolators

Dampers are passive protection devices that are very effective in anti-seismic action for new and retrofitted structures. Even though various types of dampers have been developed utilizing various technologies, they have numerous limitations related to ageing and durability (e.g. rubber-based dampers), maintenance (e.g. viscous fluid dampers), reliability in the long run (e.g. friction dampers), temperature dependent mechanical performance (e.g. rubber-based dampers, viscoelastic dampers), and geometry restoration for most dampers after a strong earthquake (Dolce et al. 2000). SMA materials have the potential to overcome many of these limitations when applied in such devices.

Clark et al. (1995) conducted experimental and analytical research on energy dissipation devices using SMAs. The basic model of the device was composed of 0.508 mm thick superelastic nitinol wire wrapped around two cylindrical support posts. There were 210 loops of

wire in the preliminary device design. The device was initially prestressed at 2.75% strain and tested under in-plane cyclic loading, which showed good hysteresis results with a little reduction in yield stress. The function of this device was analytically studied by fitting it in a 6-storey, 2-bay by 2-bay steel frame where it achieved good performance in reducing the displacement and acceleration responses by an order of ½ to ⅓ of the original structure under earthquake excitation.

Isolation devices are a special kind of dampers that introduce discontinuity between a superstructure and its substructure allowing relative horizontal displacements. They act as a filter through which the seismic energy transferred from the substructure to the superstructure is greatly reduced. The main aspect of an ideal isolator is to have a large energy dissipation capacity. Considering their full recentering and good energy dissipation capacity, SMAs seem to be very promising for use in such vibration isolation devices.

Wilde et al. (2000) proposed an isolation system for an elevated highway bridge, which consisted of a simple SMA bar combined with a laminated rubber bearing. Two isolation systems: a) proposed smart isolator (SMA), and b) conventional laminated rubber bearing with a lead core and a displacement restrainer (NZ) were considered and analyzed for North-South ground motion components of the Kobe earthquake 1995, and a sinusoidal excitation. For the smallest excitation (0.2g), a stiff connection was obtained between the pier and the deck. For a medium excitation (0.4g), an increase in the damping capacity was observed due to the stress-induced martensite transformation of SMA. For the strongest excitation (0.6g), the SMA bars provided hysteretic damping and acted as a displacement-control device due to hardening of the alloy after complete phase transformation. It was found that in each excitation the maximum relative displacement between the pier and superstructure was lower for the SMA system

compared to that of the NZ system. Also, the maximum damage energy of the bridge with the SMA system was 14% smaller than that with the NZ system.

8. Constraints of using SMA

8.1. Cost of SMA

Although there is a substantial potential of utilizing SMA in civil engineering structures, the cost of this material is a primary restraining factor to a larger implementation of SMA-based elements in structural applications. Due to the size of civil engineering structures, the forces associated with it are also large requiring substantial amount of materials, which is another hurdle for the use of the still costly SMA in civil engineering applications. A substantial portion of the cost of Ni-Ti is intrinsically related to the difficulty of processing high-strength Ni-Ti materials into particular shaped forms (Frick et al. 2004). Therefore, custom made size and machining has a considerable effect on the cost of SMAs, which may increase the price two to three times higher than that of the regular price. However, there has been a significant reduction in prices of Ni-Ti over the last ten years, from more than 1000 USD to below 150 USD per kg at present. The price is still considerably higher than that of other construction materials. The development of low-cost SMAs is essential for initiating large-scale applications. Janke et al. (2005) presented Fe-Mn-Si-X alloys as a potentially low-cost SMA. Low-cost SMA (e.g. Fe-Mn-Si-Cr) has been successfully implemented in bridge rehabilitation by Soroushian et al. (2001). Janke et al. (2005) compared the product prices of Ni-Ti with that of Fe-Mn-Si-Cr and found that the cost of Fe-based systems could only be a small fraction (1/8 to 1/12) in comparison to that of Ni-Ti systems.

The feasibility of using SMA materials and devices in full-scale construction projects has been studied by Bruno and Valente (2002). They considered various costs in their study including direct (structural, non-structural) and indirect (injuries and deaths) in the construction phase and also when induced by an earthquake. The cost of SMA-based dampers, isolation devices and bracings turned out to be of the same order as that of conventional steel devices. SMA devices have been found much preferable in the sense that they do not require additional costs such as for maintenance or replacement. The efficacy of these devices is unique in both the reduction of economic losses and minimizing human risk associated with natural disaster events.

8.2. Other issues

Both austenite and martensite-SMAs have a good potential to be used in various civil engineering applications. When using superelastic-SMA material, A_f needs to be always less than the minimum T_a to which it is exposed. If martensite-SMA is used, M_s should be set such that it is always greater than the maximum T_a to which it will be exposed. Again, designing civil engineering structures requires proper knowledge of the mechanical properties of the material to be used. The mechanical properties of SMAs largely depend on the heat-treatment temperature, where a slight variation can cause significant changes in properties. To implement a wider use of SMAs in the construction industry, manufacturers are required to produce SMAs in mass scale with proper control of its properties and transformation temperatures.

Machining large diameter bars of Ni-Ti using conventional equipment and techniques is extremely difficult due to its hardness. Although there are various ways of welding and soldering Ni-Ti, e.g. using e-beam, laser, resistance and friction welding, and brazing with Ag-based filler metals; welding Ni-Ti to steel is much more problematic because of the brittle connection around

the weld zone (Hall 2003). Weld deposits with Ni-filler metal have exhibited sufficient tensile strength allowing superelastic deformation of nitinol (Hall 2003). Threading large diameter bars reduces the strength of nitinol due to its sensitivity to notches. Although Cu-based SMAs like Cu-Zn-Al, Cu-Al-Ni are less costly, they display poor ductility. Fe-Mn-Si-based low-cost alloys have been found to exhibit good mechanical properties with a wide transformation hysteresis, good machinability and weldability as well as good workability compared to that of nitinol. Fe-based SMAs may also have good bond strength compared to that of Ni-Ti when used as reinforcing bars in RC structures. The problems related to these alloys include poor shape recovery and lower shape recovery-stress compared to that of Ni-Ti-based SMAs. A special thermomechanical treatment called 'training' must be done to improve its SME. This 'training' consists of several cycles of deformation by stress-induced martensitic transformation and subsequent reversion to austenite. This in turn will make the manufacturing process complex and increase the production cost. Improvement of SME of these alloys without training has been made possible for instance by Kajiwara and his coworkers (Baruj et al. 2002; and Dong et al. 2004).

9. Summary and concluding remarks

This paper presents the distinctive properties and several applications of SMAs in civil engineering structures. SMAs can be formed into various shapes e.g. bars, wires, plates, rings etc; and thus have the flexibility to serve various functions. SMAs' unique properties make them an ideal contender to be used as kernel components in seismic protection devices. A number of experimental and analytical studies of SMA devices (dampers and base isolators) proved them to be effective in improving the response of buildings and bridges to earthquake loading. In

particular, the recentering capability of SMA can be very efficient in reducing the cost of repairing and retrofitting of various structures after severe earthquakes. SMA has the potential to be used as reinforcement at critical regions of RC structures along with conventional steel, where the SMA is expected to yield under strains caused by seismic loads but potentially recover deformations at the end of the earthquake. Another prospective use of SMA is in prestressing, which can help a structure to actively accommodate additional loading or remedy prestress losses over time. Post-tensioning with SMA wires and tendons also proved to be a better option over conventional steel tendons in retrofitting works. The superelastic-SMAs' self repairing capabilities may be utilized to regain the preload drop in bolted joints or other types of fasteners, and thus necessary clamping forces can be provided to keep the joint members together. Although there has been substantial research work on individual components of structures utilizing SMAs, the integration of several components in a single smart structure is yet to be investigated.

Applications of SMA are numerous, while new ideas of using it in various fields and new applications are still emerging. Extensive research work still needs to be done. New SMAs need to be developed to suit the production and service temperature for industrial and building applications. The high cost of SMA is a major limiting factor for its wider use in the construction industry. Hence, the cost of the alloy needs to be considerably lowered. Fe-based SMA alloys may prove to be less costly and well suited for applications in cement-based mortar, concrete and steel. If a lower price can be ensured and more flexibility in manufacturing SMAs in various shapes and sizes is guaranteed, then SMAs have a great possibility of becoming an essential construction material in the near future. Their capability to allow the development of smart structures with active control of strength and stiffness and ability of self-healing and self-

repairing open the door for exciting opportunities, making them the construction material of the future.

References

ANSYS, Inc. Version 10.0. 2005. Southpointe, Canonsburg, PA, USA.

Auricchio, F., and Sacco, E. 1997. Superelastic shape-memory-alloy beam model. Journal of Intelligent Material Systems and Structures, **8**: 489-501.

Auricchio, F., and Taylor, R.L. 1996. Shape-memory-alloy superelastic behavior: 3D finite-element simulations. Proceedings of SPIE, Volume 2779, pp. 487-492.

Auricchio, F., Taylor, R. L., and Lubliner, J. 1997. Shape-memory-alloys: macromodelling and numerical simulations of the superelastic behaviour. Computer Methods in Applied Mechanics and Engineering, **146**: 281-312

Baruj, A., Kikuchi, T., Kajiwara, S., and Shinya, N. 2002. Effect of pre-deformation of austenite on shape-memory properties in Fe-Mn-Si-based alloys containing Nb and C. Materials Transactions, **43**: 585-588.

Bruno, S., and Valente, C. 2002. Comparative response analysis of conventional and innovative seismic protection strategies. Earthquake Engineering and Structural Dynamics, **31**: 1067-1092

Cardone, D., Dolce, M., Ponzo, F.C., and Coelho, E. 2004. Experimental behaviour of R/C frames retrofitted with dissipating and re-centering braces. Journal of Earthquake Engineering, **8**: 361-396.

Clark, P.W., Aiken, I.D., Kelly, J.M., Higashino, M. and Krumme, R. 1995. Experimental and analytical studies of shape-memory-alloy dampers for structural control. Proceedings of SPIE, Volume 2445, pp. 241-251.

Delgadillo-Holtfort, I., Kaack, M., Yohannes, T., Pelzl, J., and Khalil-Allafi, J. 2004. Ultrasonic investigation of multistage martensitic transformations in aged Ni-rich Ni-Ti shape-memory-alloys. Materials Science and Engineering A, **378**: 76-80.

DesRoches, R., and Delemont, M. 2002. Seismic retrofit of simply supported bridges using shape-memory-alloys. Engineering Structures, **24**: 325-332.

DesRoches, R., and Smith, B. 2004. Shape-memory-alloys in seismic resistant design and retrofit: a critical review of their potential and limitations. Journal of Earthquake Engineering, **8**: 415-429.

DesRoches, R., McCormick, J., and Delemont, M. 2004. Cyclic properties of superelastic shape-memory-alloy wires and bars. Journal of Structural Engineering, ASCE, **130**: 38-46.

Dolce, M. and Cardone, D. 2001. Mechanical behaviour of shape memory alloys for seismic applications 1. Martensite and austenite Ni-Ti bars subjected to torsion. International Journal of Mechanical Sciences, **43**: 2631-2656.

Dolce, M., Cardone, D., and Marnetto, R. 2000. Implementation and testing of passive control devices based on shape-memory-alloys. Earthquake Engineering and Structural Dynamics, **29**: 945-968.

Dong, Z.Z., Kajiwara, S., Kikuchi, T., and Shinya, N. 2004. High corrosion-resistance Fe-Mn-Si-based alloys exhibiting nearly perfect shape-memory-effects. Proceedings of SPIE, Volume 5387, pp. 294-301.

El-Tawil, S., and Ortega-Rosales, J. 2004. Prestressing concrete using shape-memory-alloy tendons. ACI Structural Journal, **101**: 846-851.

Frick, C.P., Ortega, A.M., Tyber, J., Gall, K., and Maier, H.J. 2004. Multiscale structure and properties of cast and deformation processed polycrystalline NiTi shape-memory-alloys. Metallurgical and Materials Transactions A, **35**: 2013-2025.

Goo, B.C., and Lexcellent, C. 1997. Micromechanics-based modeling of two-way memory-effect of a single crystalline shape-memory-alloy, Acta Materialia, **45:** 727-737.

Hall, P.C. 2003. Laser welding nitinol to stainless-steel. Proceedings of the International Conference on Shape Memory and Superelastic Technologies, California, 219-228.

Hardwicke, C.U. 2003. Recent developments in applying smart structural materials. JOM, ABI/INFORM Trade & Industry, **55:** 15-16.

Hesse, T., Ghorashi, M., and Inman, D. J. 2004. Shape-memory-alloy in tension and compression and its application as clamping-force actuator in a bolted joint: part 1– experimentation. Journal of Intelligent Material Systems and Structures, **15**: 577-587.

Hibbitt, Karlsson and Sorensen. 2003. Abaqus User's Manual, Version 6.4, Pawtucket, RI.

Hodgson, D.E. 2000. Fabrication, heat treatment and joining of nitinol components. Proceedings of the Third International Conference on Shape-Memory and Superelastic Technologies, California, pp. 11 - 24.

Huang, M., and Brinson, L.C. 1998. Multivariant model for single crystal shape-memory-alloy behaviour. Journal of the Mechanics and Physics of Solids, **46:** 1379-1409.

Humbeeck, V. 2003. Damping capacity of thermoelastic martensite in shape-memory-alloys. Journal of Alloys and Compounds, **355**: 58 –64.

Indirli, M., Castellano, M.G., Clemente, P., and Martelli, A. 2001. Demo-application of shape-memory-alloy devices: The rehabilitation of the S. Giorgio Church Bell-Tower. Proceedings of SPIE, Volume 4330, pp. 262-272.

Janke, L., Czaderski, C., Motavalli, M., and Ruth, J. 2005. Applications of shape-memory-alloys in civil engineering structures-overview, limits and new ideas. Materials and Structures, **38**: 578-592.

Jung, M.S. 2006. Microactuator and fluid transfer apparatus using the same. United States Patent no. 7128403.

Kannel, J., French, C., and Stolarski, H. 1997. Release methodology of strands to reduce end cracking in pretensioned concrete girders. PCI Journal, **42**: 42-54.

Khantachawana, A., Miyazaki, S., Iwai, H., and Kohl, M. 1999. Effect of heat-treatment on the texture and anisotropy of transformation strain in Ti-Ni-Fe rolled thin plates. Materials Science and Engineering A, **A273-275:** 763-768.

Liang, C., and Rogers, C.A. 1990. One-dimensional thermomechanical constitutive relations for shape-memory materials. Structural Dynamics & Materials Conference, pp. 16-28.

Lim, T. J., and McDowell, D.L. 1999. Mechanical behaviour of an Ni-Ti shape-memory-alloy under axial-torsional proportional and nonproportional loading. Journal of Engineering Materials and Technology, Transactions of the ASME, **121**: 9-18.

Liu, Y. 2003. Mechanical and thermomechanical properties of a $Ti_{50}Ni_{25}Cu_{25}$ melt spun ribbon. Materials Science and Engineering A, **354**: 286-291.

Liu, Y., and Favier, D. 2000. Stabilisation of martensite due to shear deformation via variant reorientation in polycrystalline NiTi. Acta Materialia, **48**: 3489-3499.

Liu, Y., Xie, Z., and Van Humbeeck, J. 1999. Cyclic deformation of NiTi shape-memory-alloys. Materials Science and Engineering A, **A273-275**: 673-678.

Liu, Y., Xie, Z., Humbeeck, J.V. and Delaey, L. 1998. Asymmetry of stress–strain curves under tension and compression for NiTi shape-memory-alloys. Acta Materialia, **46**: 4325-4338.

Maji, A.K., and Negret, I. 1998. Smart prestressing with shape-memory-alloy. Journal of Engineering Mechanics, **124**: 1121-1128.

Manach, P.-Y., and Favier, D. 1997. Shear and tensile thermomechanical behavior of near equiatomic NiTi alloy. Materials Science & Engineering A, **A222**: 45-57.

McNaney, J.M., Imbeni, V., Jung, Y., Papadopoulos, P., and Ritchie, R.O. 2003. An experimental study of the superelastic effect in a shape-memory nitinol alloy under biaxial loading. Mechanics of Materials, **35**: 969–986.

Miller, A. 2005. Multi-fastener surgical apparatus and method. United States Patent no. 6837893.

Miyazaki, S., Imai, T., Igo, Y., and Otsuka, K. 1986. Effect of cyclic deformation on the pseudoelasticity characteristics of Ti–Ni alloys. Metallurgical Transactions. A, **17A**: 115–120.

Norton, K.H. 1998. Disk drives. United States Patent no. 5808837.

Ocel, J., DesRoches, R., Leon, R. T., Hess, W. G., Krumme, R. Hayes, J. R., and Sweeney, S. 2004. Steel beam-column connections using shape-memory-alloys. Journal of Structural Engineering, ASCE, **130**: 732-740.

Orgeas, L., and Favier, D. 1995. Non-symmetric tension-compression behaviour of NiTi-alloy. Journal De Physique. IV: JP, **5**: 605-610.

Orgeas, L., Liu, Y., and Favier, D. 1997. Experimental study of mechanical hysteresis of NiTi during ferroelastic and superelastic deformation. Journal De Physique. IV : JP, **7:**C5-477-C5-482.

Otsuka, K. and Wayman, C.M. 1999. Shape-memory materials, Cambridge University Press, Cambridge.

Patoor, E., Eberhardt, A., and Berveiller, M. 1994. Micromechanical modelling of the shape behaviour. ASME, AMD, Mechanics of Phase Transformations and Shape-Memory-Alloys, Volume 189, pp. 23-37.

Recarte, V., Pérez-Landazábal, J.I., Rodríguez, P.P., Bocanegra, E.H., No, M.L., and Juan, J.S. 2004. Thermodynamics of thermally induced martensitic transformations in Cu–Al–Ni shape-memory-alloys. Acta Materialia, 52: 3941-3948.

Rejzner, J., Lexcellent, C., and Raniecki, B. 2002. Pseudoelastic behaviour of shape-memory-alloy beams under pure bending: Experiments and modelling. International Journal of Mechanical Sciences, **44**: 665-686.

Salichs, J., Hou, Z., and Noori, M. 2001. Vibration suppression of structures using passive shape-memory-alloy energy dissipation devices. Journal of Intelligent Material Systems and Structures, **12**: 671-680.

Schiff, A. 1998. Hyogoken-Nanbu (Kobe) Earthquake of January 17, 1995, Lifeline Performance. American Society of Civil Engineers.

SeismoStruct Help file. 2004. http://www.seismosoft.com/SeismoStruct/index.htm, visited on Jan 2006.

Song, G., Ma, N., and Li, H.-N. 2006. Application of shape-memory-alloys in civil structures. Engineering Structures, **28**: 1266-1274.

Soroushian, P., Ostowari, K., Nossoni, A., and Chowdhury, H. 2001. Repair and strengthening of concrete structures through application of corrective posttensioning forces with shape-memory-alloys. Transportation Research Record, **1770**: 20-26.

Special Metals. 2006. http://www.shape-memory-alloys.com/data_nitinol.htm#nitife, visited on May 2006.

Strnadel, B., Ohashi, S., Ishihara, T., Ohtsuka, H., and Miyazaki, S. 1995. Cyclic stress-strain characteristics of Ti-Ni and Ti-Ni-Cu shape-memory-alloys. Materials Science and Engineering: A, **202**: 148-156.

Tanaka, K., and Nagaki, S. 1982. Thermomechanical desription of materials with internal variables in the process of phase transitions. Ingenieur-Archiv, **51**: 287-299.

Ullakko, K. 1996. Magnetically controlled shape-memory-alloys: a new class of actuator materials. Journal of Materials Engineering and Performance, **5**: 405-409.

Vivet, A., Orgeas, L., Lexcellent, C., Favier, D., and Bernardini, J. 2001. Shear and tensile pseudoelastic behaviours of CuZnAl single crystals. Scripta Materialia, **45**: 33-40.

Wang, H., 2004. A study of RC columns with shape-memory-alloy and engineered cementitious composites. M.Sc. Thesis, University of Nevada, Reno.

Wang, Y.Q., Zheng, Y.F., Cai, W., and Zhao, L.C. 1999. The tensile behavior of $Ti_{36}Ni_{49}Hf_{15}$ high temperature shape-memory-alloy. Scripta Materialia, **40**: 1327–1331.

Wilde, K., Gardoni, P., and Fujino, Y. 2000. Base isolation system with shape-memory-alloy device for elevated highway bridges. Engineering Structures, **22**: 222-229.

Wilson, J.C. and Wesolowsky, M.J. 2005. Shape-memory-alloys for seismic response modification: A state-of-the-art review. Earthquake Spectra, **21**: 569-601.

Table 1. Chemical compositions and transformation temperatures of various SMAs (for stress-free state).

Alloy	Composition	Fabrication process	M_f	M_s	A_s	A_f
	Percentage		K	K	K	K
Ni-Ti (Manach and Favier 1997)	50.5-49.5	hot-rolled and subsequently cold-rolled with intermediate annealing	277.0	306.0	317.0	335.0
Ni-Ti (Delgadillo-Holtfort et al. 2004)	50.8-49.2	Annealed followed by water quenching	227.0	252.0	270.0	284.0
Ni-Ti (Hesse et al. 2004)	55.7-44.3	Unannealed	204.0 ± 2.0	287.0 ± 1.0	264.0 ± 2.0	295.0 ± 2.0
		Annealed	233.0 ± 2.0	278.0 ± 2.0	291.0 ± 0.3	324.0 ± 1.5
Ni-Ti (Strnadel et al. *1995)*	50.9-49.1	Vacuum annealed followed by water quenching	157.4	242.5	275.1	317.8
	50.5-49.5		195.4	254.7	282.2	326.2
	50.0-50.0		245.2	310.7	321.4	351.0
Ni-Ti-Cu (Strnadel et al. *1995)*	40.0-50.0-10.0		294.1	314.6	325.9	339.8
Cu-Zn-Al (Vivet et al., 2001)	25.6-4.2-70.2	Annealed followed by aging in a quenching bath	288.5	292.3	293.2	298.3
Cu-Al-Ni (Recarte et al. 2004)	82.0-14.0-4.0	Annealed followed by water quenching	252.0	246.0	274.0	285.0
Cu–Al–Be (Rejzner et al. 2002)	11.6-0.6-87.8	—	157.0	179.0	169.0	195.0
Ni-Ti-Fe (Special Metals 2006)	53.5-45-1.5	Cold-drawn	—	—	263.0 ± 5.0	283.0 ± 5.0
Ti-Ni-Hf (Wang et al. 1999)	36-49-15	Rot-rolled	421.0	452.0	489.0	504.0

Table 2. Mechanical properties of Ni-Ti alloy.

Property		Phase	Unit	Range
Under tension (Manach and Favier 1997, DesRoches et al. 2004, Otsuka and Wayman 1999, Rejzner et al. 2002)	Young's modulus, E_y	Austenite	GPa	30-98
		Martensite	GPa	21-52
	Yield strength, f_y	Austenite	MPa	100-800
		Martensite	MPa	50-300
	Ultimate strength, f_u	Austenite	MPa	800-1900
		Martensite	MPa	800-2000
	Elongation at failure, ε_u	Austenite	Percentage	5-50
		Martensite	Percentage	20-60
	Recovered pseudoelastic strain, ε_{PI}	Austenite	Percentage	≤ 8
	Maximum recovery-stress, f_{PI}	Austenite	MPa	600-800
Under compression (Liu et al. 1998, Orgeas and Favier D 1995, Lim and McDowell 1999)	Young's modulus, E_y	Austenite	GPa	56-69
		Martensite	GPa	20-80
	Yield strength, f_y	Austenite	MPa	550-800
		Martensite	MPa	125-190
	Ultimate strength, f_u	Austenite	MPa	1500
		Martensite	MPa	1800-2120
	Elongation at failure, ε_u	Austenite	Percentage	—
		Martensite	Percentage	17-24
	Recovered pseudoelastic strain, ε_{PI}	Austenite	Percentage	3-6
	Maximum recovery-stress, f_{PI}	Austenite	Percentage	650-820
Under shear (Manach and Favier 1997, Delgadillo-Holtfort et al. 2004, Liu and Favier 2000)	Shear modulus, G_y	Austenite	GPa	18-25
		Martensite	GPa	25-40
	Yield strength, τ_y	Austenite	MPa	186
		Martensite	MPa	42-100
	Ultimate strength, τ_u	Austenite	MPa	>515
		Martensite	MPa	<515
	Elongation at failure, γ_u	Austenite	Percentage	≤ 40
		Martensite	Percentage	≤ 40
	Recovered pseudoelastic strain, γ_{PI}	Austenite	Percentage	6
	Maximum recovery-stress, τ_{PI}	Austenite	Percentage	300
Under torsion (McNaney et al. 2003, Lim and McDowell 1999, Dolce and Cardone 2001)	Shear modulus, G_y	Austenite	GPa	6-28
		Martensite	GPa	4-9
	Yield strength, τ_y	Austenite	MPa	220-350
		Martensite	MPa	88
	Ultimate strength, τ_u	Austenite	MPa	>500
		Martensite	MPa	210-380
	Elongation at failure, γ_u	Austenite	Percentage	10 - >24
		Martensite	Percentage	—
	Recovered pseudoelastic strain, γ_{PI}	Austenite	Percentage	6
	Maximum recovery-stress, τ_{PI}	Austenite	Percentage	270-500

Table 3. Mechanical properties of various SMAs.

Property	E_y Austenite	E_y Martensite	f_y Austenite	f_y Martensite	Lower plateau stress	f_u Austenite	f_u Martensite	ε_u Martensite	ε_{PI}	f_{PI}	Residual-strain
	GPa	GPa	MPa	MPa	MPa	MPa	MPa	%	%	MPa	%
Cu-Zn-Al (Otsuka and Wayman 1999)	70-100	70	150-350	80-300	-	400-900	700-800	10-15	3.5		-
Ni-Ti-Fe (Special Metals 2006)	-	-	≥688	-	≥447	≥1443	-	≥10	≤ 8.0	-	0.5
Cu-Al-Ni (Otsuka and Wayman 1999)	80-100	80	150-300	150-300	-	500-1200	1000-1200	8-10	2.0		-
Ti-Ni-Cu (Liu 2003)	15-16	-	300	-	-	-	-	-	4.5-7.5	280-700	0.6-3.2
Cu-Al-Be (Rejzner et al. 2002)	25	25	110-210		80-170	-	-	-	8.0-10.0	220	-
Ti-Ni-Hf (Wang et al. 1999)	12-19	15	420-620	430-460	-	907-1227	1227	10-30	≥ 3.0		-

List of Figures

Fig. 1. Alam, Youssef and Nehdi

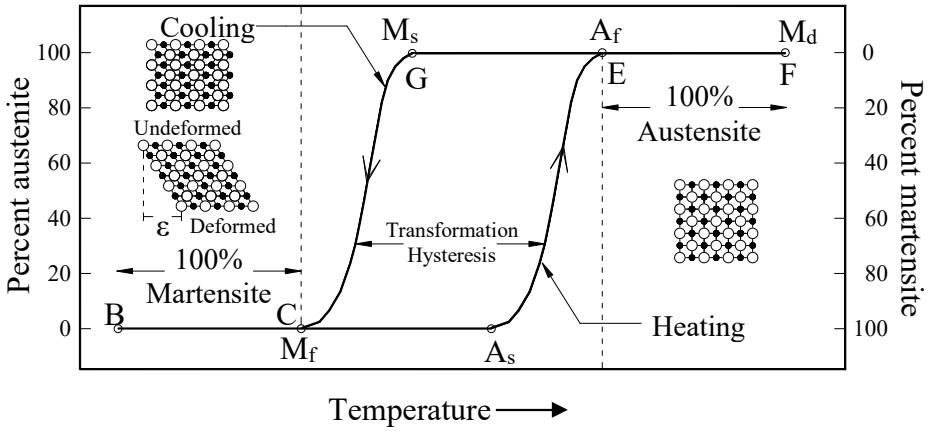

Fig. 2. Alam, Youssef and Nehdi

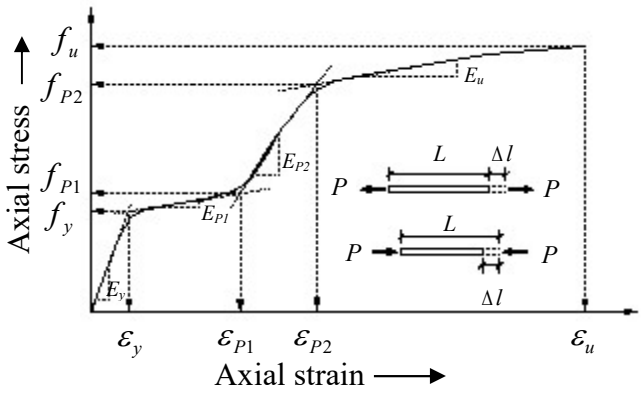

Fig. 3. Alam, Youssef and Nehdi

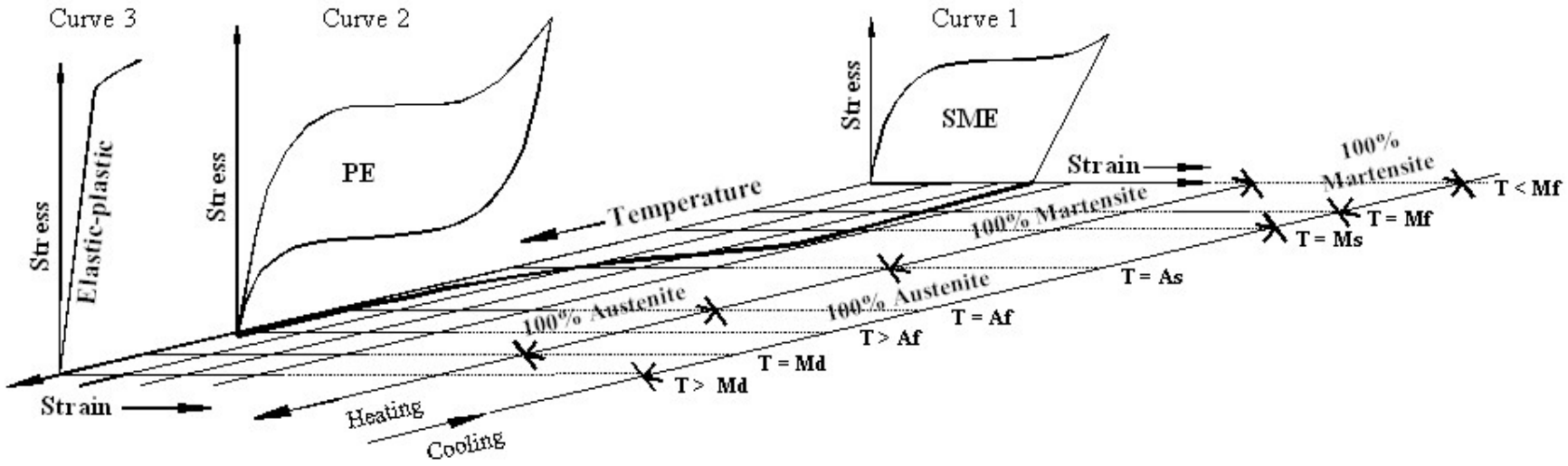

Fig. 4. Alam, Youssef and Nehdi

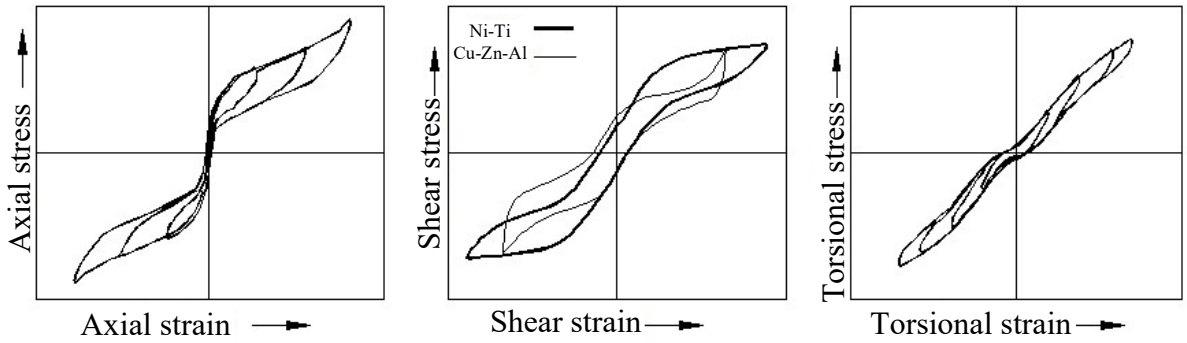

Fig. 5. Alam, Youssef and Nehdi

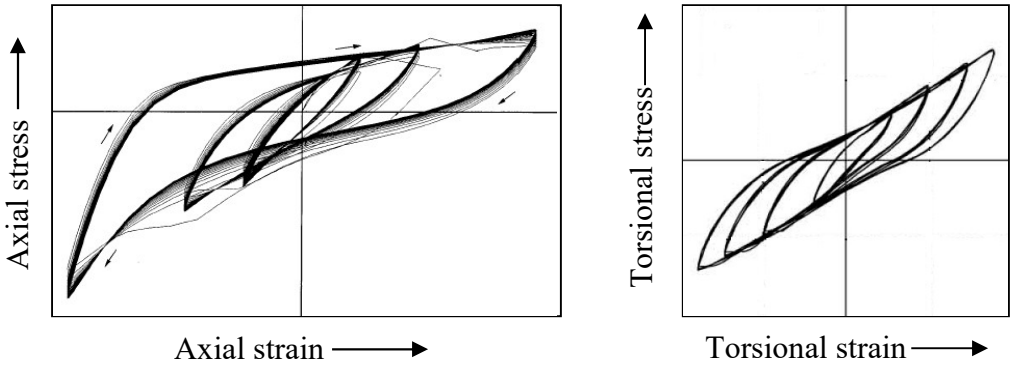

Fig. 6. Alam, Youssef and Nehdi